Accepted Manuscript

Synthesis, optical characterization, and solvatochromism study of new two-photon absorption compounds

Yan-Tao Zhou, Zhi-Bin Cai, Yu-Lu Pan, Li Bai, Guo-Chuang Zheng, Sheng -Li Li, Yu-Peng Tian

PII: S0040-4020(16)30163-6

DOI: 10.1016/j.tet.2016.03.030

Reference: TET 27570

To appear in: *Tetrahedron*

Received Date: 22 January 2016

Revised Date: 2 March 2016

Accepted Date: 8 March 2016

Please cite this article as: Zhou Y-T, Cai Z-B, Pan Y-L, Bai L, Zheng G-C, Li S-L, Tian Y-P, Synthesis, optical characterization, and solvatochromism study of new two-photon absorption compounds, *Tetrahedron* (2016), doi: 10.1016/j.tet.2016.03.030.

Graphical abstract

The new donor-π-acceptor / acceptor-π-acceptor compounds exhibit strong up-converted fluorescence, obvious solvatochromic effects, and the largest σ value in various solvents, which provide a promising alternative as a polarity-sensitive two-photon fluorescent probe.

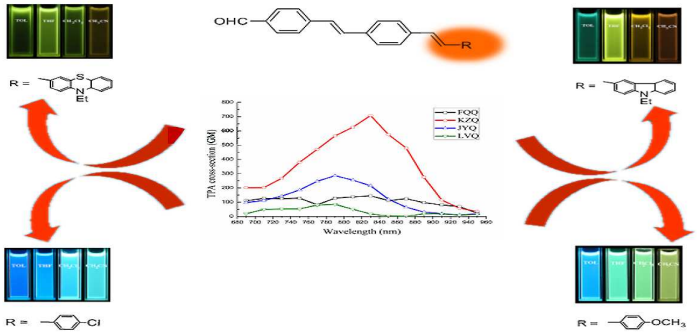

Synthesis, optical characterization, and solvatochromism study of new two-photon absorption compounds

Yan-Tao Zhou [a], Zhi-Bin Cai [a,*], Yu-Lu Pan [a], Li Bai [a], Guo-Chuang Zheng [a], Sheng-Li Li [b] and Yu-Peng Tian [b]

[a] *College of Chemical Engineering, Zhejiang University of Technology, Hangzhou 310014, PR China*

[b] *Department of Chemistry, Anhui Province Key Laboratory of Functional Inorganic Materials, Anhui University, Hefei 230039, PR China*

Abstract

The new donor-π-acceptor / acceptor-π-acceptor compounds (**FQQ**, **KZQ**, **JYQ**, and **LVQ**) were facilely synthesized and characterized by infrared, proton nuclear magnetic resonance, mass spectrometry, and elemental analysis. Their UV-visible absorption, one-photon excited fluorescence, two-photon absorption, and two-photon excited fluorescence were systematically investigated in different solvents. The experiment results indicate that all these compounds exhibit relatively strong up-converted fluorescence and obvious solvatochromic effects. **KZQ** shows the largest σ value of 707 GM in THF upon 830 nm excitation. Its excellent optical properties provide a promising alternative as a polarity-sensitive two-photon fluorescent probe. Aided with the quantum chemical density functional theory calculations, the relationships between the structures and the properties were studied.

*Corresponding author. Tel. : +86 571 88320891.

E-mail address: caizbmail@126.com (Z.-B. Cai).

Keywords: Optical property; Solvatochromism; Two-photon absorption compound; Synthesis

1. Introduction

Two-photon absorption (TPA) is a third-order nonlinear optical process involving simultaneous absorption of two photons to reach the excited state. TPA materials are of interest in current research due to their potential applications in photodynamic therapy[1], scanning excitation microscopy[2], up-converted lasing and three-dimensional optical data storage[3], etc. Especially, bioimaging techniques based on TPA methods are superior to those based on one-photon absorption[4] owing to their in-depth penetration, less cell damage, and higher spatial resolution[5]. Therefore, to fully realize these applications, great effort has been focused on the design and synthesis of organic materials with high TPA cross-section (σ)[6]. Generally, there are several factors on increasing σ values: (1) the efficiency of intramolecular charge transfer (ICT)[7]; (2) the strength of the donor and acceptor[8]; (3) the character of the conjugated bridge[9]; (4) the coplanarity of the molecule structure[10]; (5) the alternation of the conjugation length[11]; (6) the dimensionality of the charge transfer network[12]. Up till now, many organic materials have been synthesized with high σ as the following structure types: dipolar D-π-A (A = acceptor, D = donor, and π = conjugated bridge)[13], quadrupolar D-π-D / A-π-A and D-π-A-π-D / A-π-D-π-A[14], octupoles[15], and TPA oligomers / polymers[16]. Among them, organic molecules with D-π-A system are the most extensively studied because their spectra and energy gaps can be tuned by controlling the ICT from the conjugated electron donors to the electron acceptors, which plays an important role in the determination of the photophysical properties. However, as far as the practical applications be concerned, it is still a challenge by now that how to design and facilely synthesize dipolar molecules with the low molecular weight, the small molecular volume, and the large σ.

It is well-accepted that 9-ethyl-9*H*-carbazole and 10-ethyl-10*H*-phenothiazine, as a class of large electron-rich heterocyclic structure, have strong electron-donating

ability[17], and methoxy is also a kind of effective electron-donating group[18]. Though formyl has a relatively strong electron-withdrawing ability, a few examples that formyl was studied as a type of electron acceptor in TPA materials have been reported. We had previously synthesized a series of A-D-A molecules with a formyl moiety, and it is proved that formyl can act as a good electron acceptor[19]. Herein, based on the above considerations, we strategically designed three new D-π-A compounds (**FQQ**, **KZQ**, and **JYQ**) and one new A-π-A (**LVQ**) counterpart, whose chemical structures were illustrated in Scheme 1. Four new target compounds were facilely synthesized by the following three-step reactions: (1) Arbuzov reaction; (2) solvent-free Horner-Wadsworth-Emmons (HWE) reaction; (3) Mizoroki-Heck reaction. They were characterized by IR, ^{1}H NMR, MS, and elemental analysis. Their linear photophysical characteristics were performed in different organic solvents and the TPA properties were investigated by means of the two-photon fluorescence spectroscopy. To well understand the underlying mechanisms of TPA properties, the theoretical calculations were employed to investigate the structure-property relationships of the target molecules by density functional theory (DFT) calculation approaches[20]. Furthermore, four target compounds showed obvious solvatochromic effects[21] and large Stokes shifts upon increasing the polarity of solvents mainly due to ICT. The optical characterization and investigation of TPA properties show that the target compounds could provide promising alternatives as polarity-sensitive two-photon fluorescent probes.

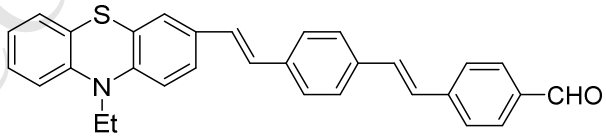

FQQ

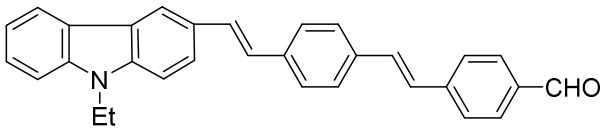

KZQ

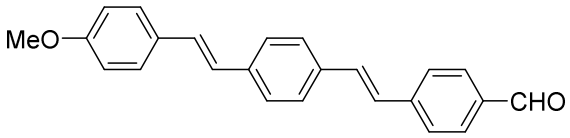

JYQ

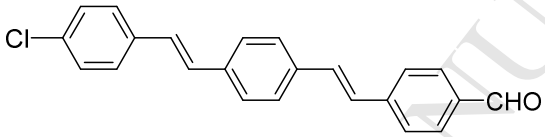

LVQ

Scheme 1. Molecular structures of the target compounds (**FQQ**, **KZQ**, **JYQ**, and **LVQ**).

2. Results and discussion

2.1. Synthesis and characterization

The synthesis of the target compounds (**FQQ**, **KZQ**, **JYQ**, and **LVQ**) is relatively straightforward as outlined in Scheme 2. The 10-ethyl-10*H*-phenothiazine-3-carboxaldehyde[23] (**1a**) and 9-ethyl-9*H*-carbazole-3-carboxaldehyde[24] (**1b**) were synthesized efficiently by Vilsmeier reaction according to the references. Meanwhile, we used [(4-ethenylphenyl)methyl]phosphonic acid diethyl ester as the starting material to realize the synthesis of the phosphonate compound (**LSZ**) according to the literature[25], which was then reacted with the aromatic aldehydes (**1a**-**1d**) by the solvent-free HWE reaction to form the trans-alkenes (**2a**-**2d**). Among these important intermediates, **2a**

was synthesized and reported for the first time by our research group. The solvent-free HWE reaction is simple, safe, and environmentally friendly. And its additional advantage of high *E*-selectivity make this method a candidate for not only laboratory use but also widespread industrial applications. By following Mizoroki-Heck reaction, the target compounds were accomplished in 61%-73% yields. In ^{1}H NMR spectra, one can see the chemical shifts (δ) of **2a**-**2d** at 6.73-6.75 (J_1 = 17.6-17.7 Hz, J_2 = 10.9-11.0 Hz, 1H) , 5.84-5.87 (J = 17.6-17.7Hz, 1H), and 5.26-5.28 (J = 11.0-11.1 Hz, 1H) show the existence of the terminal carbon-carbon double bond. The *E*-configurations of the carbon-carbon double bonds are certified by the coupling constants J = 16.3-16.5 Hz for the olefinic AB spin systems. Meanwhile, the δ values at 9.99-10.0 (s, 1H) indicate the existence of the formyl group. In the FT-IR spectra of the target compounds, the characteristic absorption peaks appearing at 1693-1700 cm^{-1} are the stretch vibration absorption of the carbonyl group, and the characteristic absorption peaks appearing at 1589-1597 cm^{-1} and 957-968 cm^{-1} illustrate the stretch and bending vibration of the *E*-configurations of the carbon-carbon double bonds, respectively.

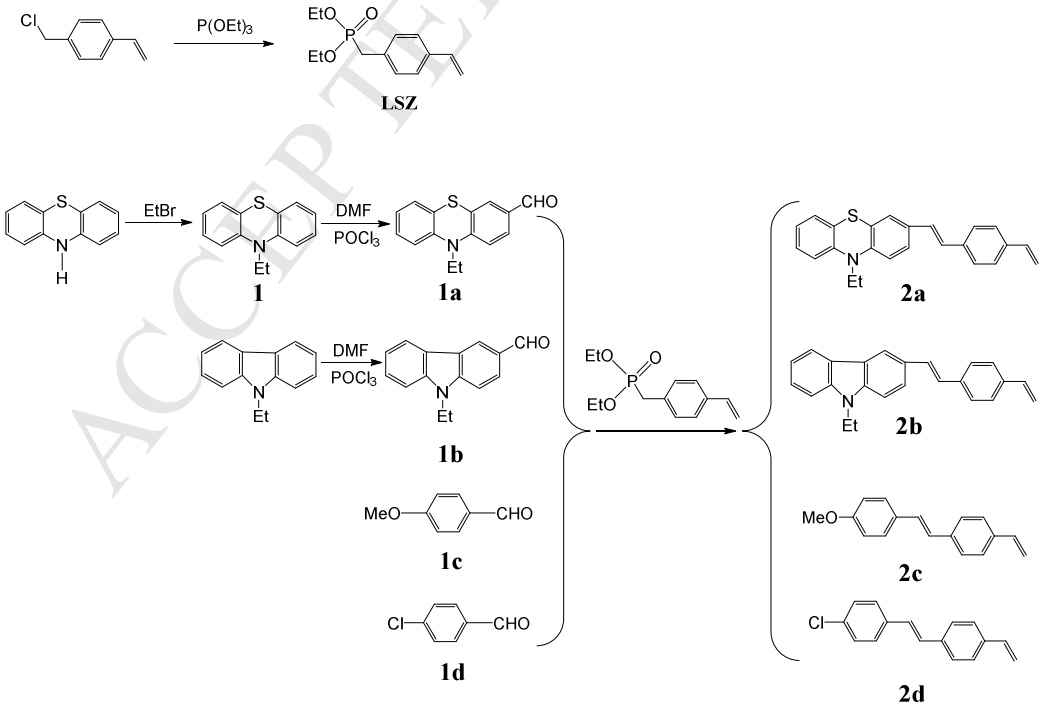

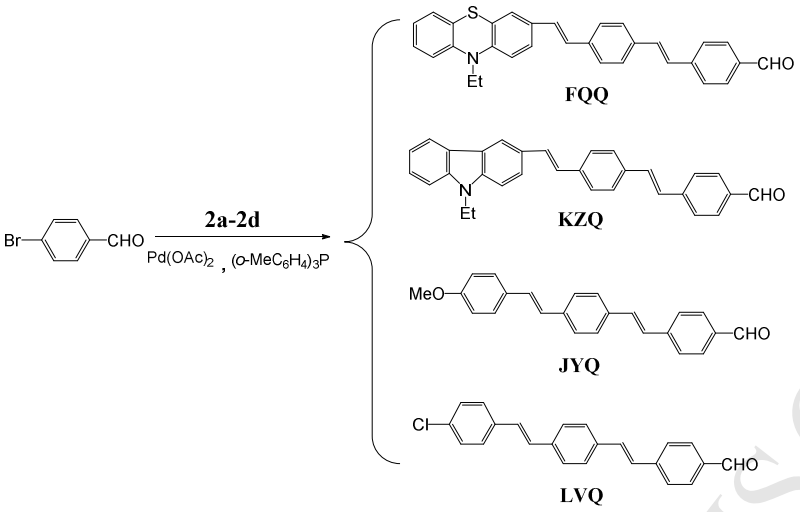

Scheme 1. Synthesis of the target compounds (**FQQ**, **KZQ**, **JYQ**, and **LVQ**).

2.2. One-photon absorption and fluorescence properties

The one-photon absorption and fluorescence properties of the target compounds in four solvents of different polarity are listed in Table 1. To further investigate the spectra relationships of the compounds, the corresponding one-photon absorption and fluorescence spectra of the target compounds are depicted in Fig. 1, Fig. 2, and Fig. 3.

Table 1. Linear and nonlinear optical properties of the target compounds (**FQQ**, **KZQ**, **JYQ**, and **LVQ**).

Compound	Solvent	λ_{max}^{abs} [a] (nm)	$10^{-4}\varepsilon$ [b] (mol^{-1} L cm^{-1})	λ_{max}^{OPEF} [c] (nm)	$\Delta\nu$ [d] (cm^{-1})	ϕ [e]	λ_{max}^{TPEF} [f] (nm)	σ [g] (GM)
FQQ	TOL	405	2.15	510	5083	0.28	561	118
	THF	407	4.80	520	5339	0.18	572	145
	CH_2Cl_2	401	3.58	527	5962	0.12		

	CH_3CN	399	3.38	542	6612	0.09		
KZQ	TOL	402	4.53	475	3823	0.88	520	448
	THF	399	4.76	528	6123	0.48	563	707
	CH_2Cl_2	400	4.89	548	6752	0.29		
	CH_3CN	394	4.58	563	7619	0.08		
JYQ	TOL	384	10.67	467	4628	0.97	505	138
	THF	379	6.22	487	5851	0.51	525	286
	CH_2Cl_2	381	10.58	508	6562	0.43		
	CH_3CN	376	9.49	530	7728	0.33		
LVQ	TOL	374	7.53	446	4245	0.68	489	55
	THF	372	13.59	448	4560	0.63	493	85
	CH_2Cl_2	372	11.73	454	4855	0.65		
	CH_3CN	373	9.37	464	5257	0.60		

[a] Maximum linear absorption wavelength, $c = 1\times10^{-5}$ mol L^{-1}.

[b] Maximum molar absorption coefficient.

[c] Maximum one-photon excited fluorescence wavelength, $c = 1\times10^{-6}$ mol L^{-1}.

[d] Stokes shift.

[e] Fluorescence quantum yield, measured by using quinine sulfate in 0.5 mol L^{-1} sulfuric acid as the standard ($\Phi = 0.546$[26]).

[f] Maximum two-photon excited fluorescence wavelength, $c = 1\times10^{-3}$ mol L^{-1}.

[g] Two-photon absorption cross-section, 1 GM = 1×10^{-50} cm^4 s $photon^{-1}$.

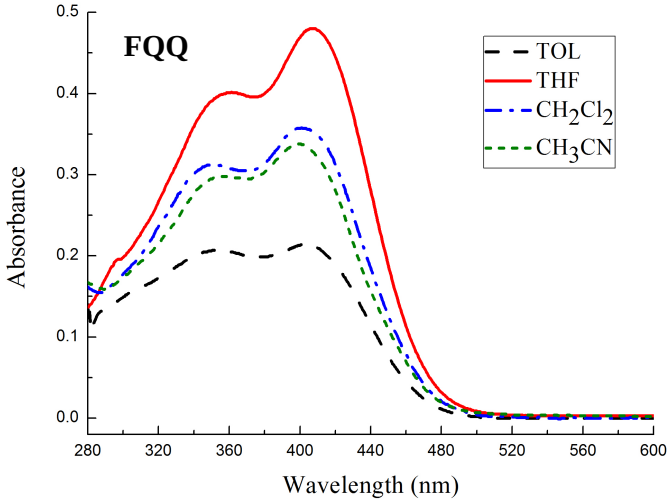
FQQ
TOL
THF
CH_2Cl_2
CH_3CN
Absorbance
Wavelength (nm)
0.0
0.1
0.2
0.3
0.4
0.5
280
320
360
400
440
480
520
560
600

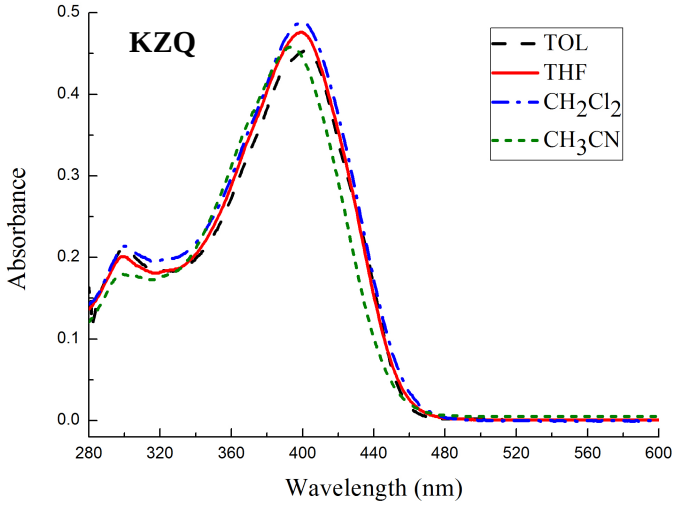
KZQ
TOL
THF
CH_2Cl_2
CH_3CN
Absorbance
Wavelength (nm)
0.0
0.1
0.2
0.3
0.4
0.5
280
320
360
400
440
480
520
560
600

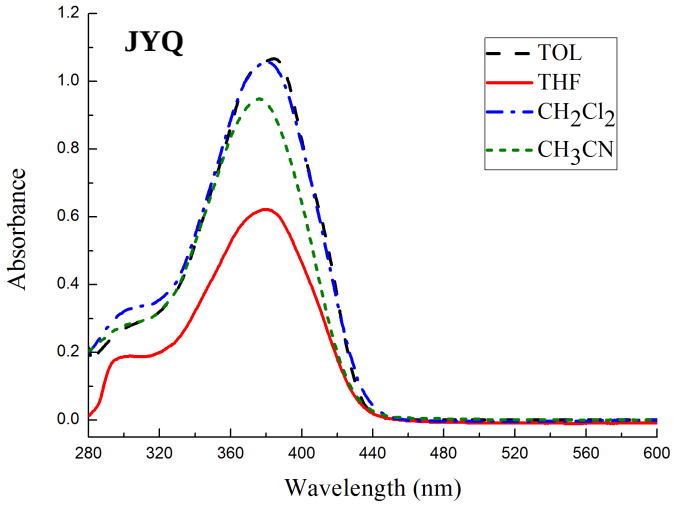

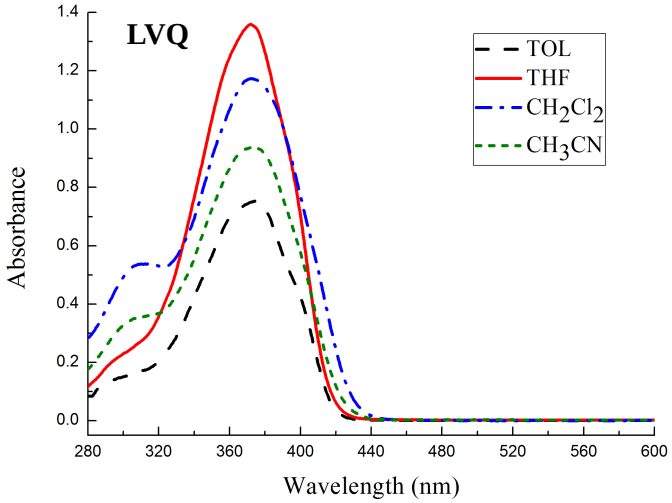

Fig. 1. One-photon absorption spectra of the target compounds (**FQQ**, **KZQ**, **JYQ**, and **LVQ**) in different solvents with a concentration of 1×10^{-5} mol L^{-1}.

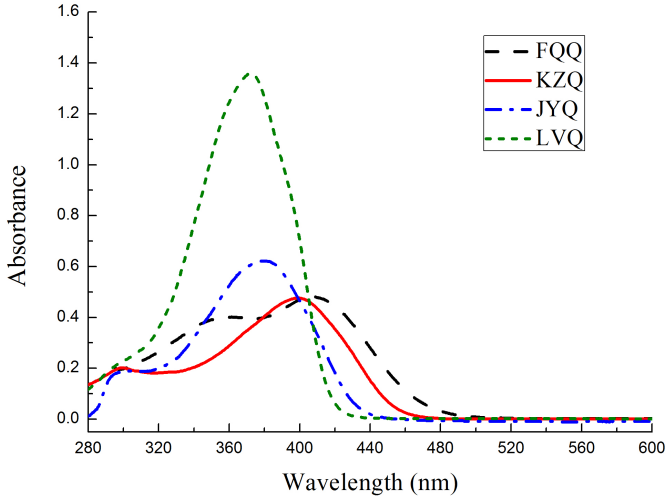

Fig. 2. One-photon absorption spectra of the target compounds (**FQQ**, **KZQ**, **JYQ**, and **LVQ**) in THF with a concentration of 1×10^{-5} mol L^{-1}.

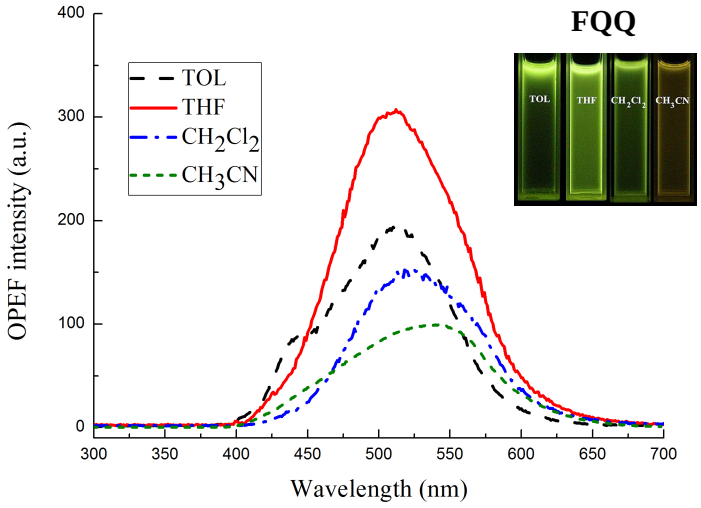

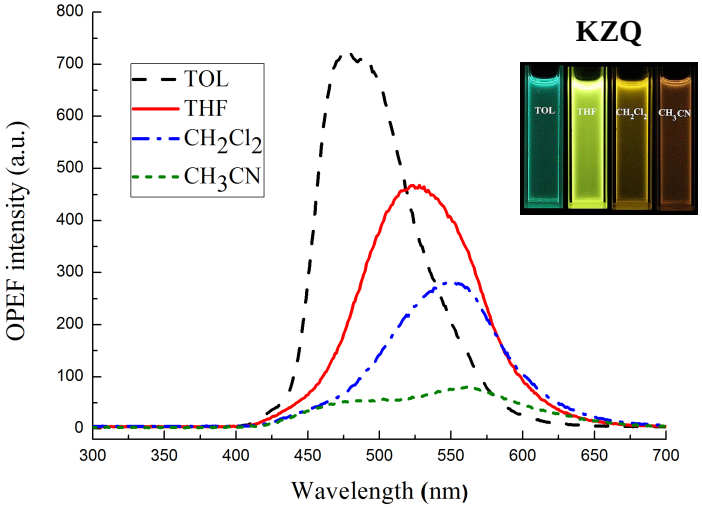
KZQ
TOL
THF
CH_2Cl_2
CH_3CN
OPEF intensity (a.u.)
Wavelength (nm)
0
100
200
300
400
500
600
700
800
300
350
400
450
500
550
600
650
700

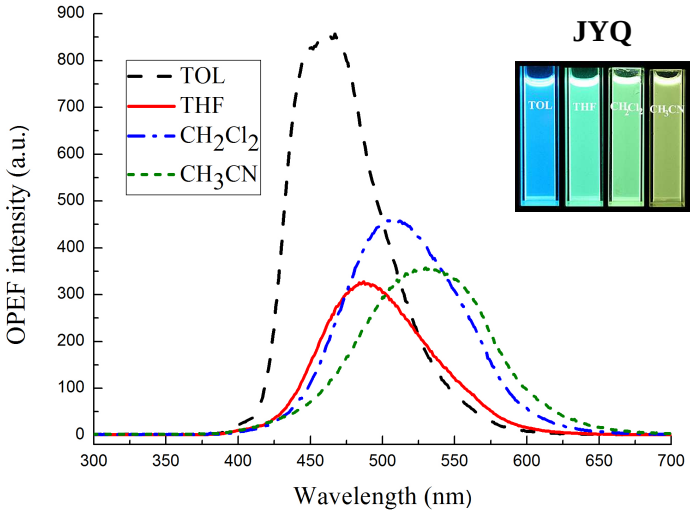
JYQ
TOL
THF
CH_2Cl_2
CH_3CN
OPEF intensity (a.u.)
Wavelength (nm)
0
100
200
300
400
500
600
700
800
900
300
350
400
450
500
550
600
650
700

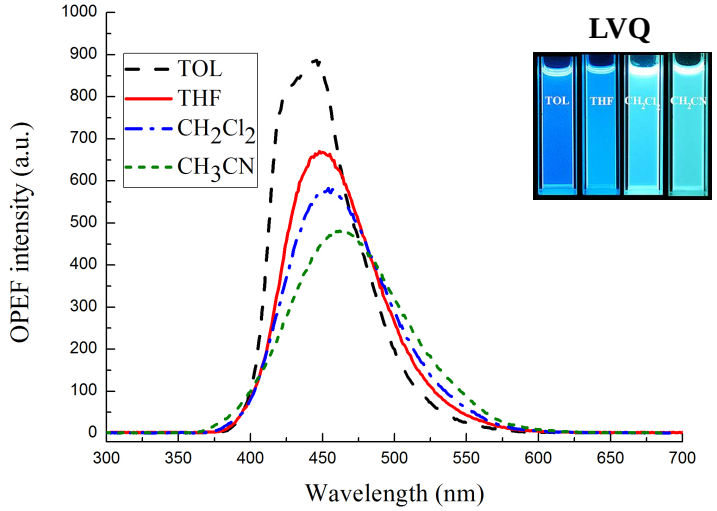

Fig. 3. One-photon fluorescence spectra of the target compounds (**FQQ**, **KZQ**, **JYQ**, and **LVQ**) in different solvents with a concentration of 1×10^{-6} mol L^{-1}.

As shown in Fig. 1, all of the compounds show two absorption bands in the range of 290-360 nm and 372-407 nm. The low-energy band originates from the ICT transition, while the high-energy band is assigned to the π-π* transition of the phenothiazine ring (**FQQ**), the carbazole ring (**KZQ**), and the benzene ring (**JYQ**, **LVQ**). With increasing solvent polarity from TOL to CH_3CN, the absorption peak positions (λ_{max}^{abs}) of **FQQ**, **KZQ**, **JYQ**, and **LVQ** only have a little variation (< 8 nm). It can be seen from Fig. 2 that the λ_{max}^{abs} exhibits an obvious red shift from **LVQ** to **FQQ** (**LVQ < JYQ < KZQ < FQQ**). The reason for this characteristic is that phenothiazine is a kind of nitrogen and sulfur-containing heterocyclic unit, and carbazole is a kind of nitrogen-containing heterocyclic unit, which extend the conjugation length of the system and lead to lower electronic transition energy between the ground state and the excited state. Note that the maximum molar absorptivities (ε_{max}) of **LVQ** and **JYQ** are much larger than those of **FQQ** and **KZQ**, which implies that the light absorbing ability of the compounds with heterocyclic donors is relatively weak.

As shown in Fig. 3 and listed in table 1, all the four compounds emit one-photon excited fluorescence (OPEF) between 380 and 680 nm under the excitation at their maximum absorption wavelengths. The compounds exhibit solvatochromic behavior in different polar solvents. Upon increasing solvent polarity, the OPEF maxima (λ_{max}^{OPEF}) of **FQQ**, **KZQ**, **JYQ**, and **LVQ** show obvious bathochromic shifts. For example, the λ_{max}^{OPEF} of **KZQ** shows a red-shift by 88 nm that exhibits a greater sensitivity to each solvent than the other compounds (**FQQ**, **JYQ**, and **LVQ**). The Stokes shifts ($\Delta\nu$) also show a tendency to monotonically increase with increasing the polarity of solvents from TOL to CH_3CN. These observations can be due to the following reasons: the molecular polarity of the excited state is larger than that of the ground state, as the enhanced dipole-dipole interactions caused by increasing the polarity of the solutes and / or solvents will lead to a more significant energy level decrease for the excited state. The fluorescence quantum yields (Φ) of the four compounds in different solvents were determined by using quinine sulfate in 0.5 mol L^{-1} sulfuric acid as the standard. In low-polarity TOL, the Φ show a sequence of **JYQ** (0.97) > **KZQ** (0.88) > **LVQ** (0.68) > **FQQ** (0.28). Upon increasing solvent polarity, the Φ of **LVQ** changes slightly, while the Φ of **FQQ**, **KZQ**, and **JYQ** decrease consistently and significantly. Especially, the Φ of **FQQ** and **KZQ** are almost quenched in highly polar CH_3CN. The above results indicate that **FQQ**, **KZQ**, and **JYQ** have much stronger ICT than **LVQ**.

The large values of $\Delta\nu$ are observed for the target compounds in all four solvents due to the strong solvent-solute dipole-dipole interactions, a manifestation of the large dipole moments and orientation polarizability. As described above, the fluorescence spectra show the large $\Delta\nu$ which depend on the solvent polarity. The significant solvatochromism is observed, suggesting a large change in the dipole moment between the ground and the excited state. The Lippert-Mataga equation is the most widely used equation to evaluate the dipole moment changes of the materials with photoexcitation:[27]

$$\Delta v = \frac{2\Delta f}{4\pi\varepsilon_0 hca^3}(\mu_e - \mu_g)^2 + const \qquad (1)$$

$$\Delta f = \frac{\varepsilon - 1}{2\varepsilon + 1} - \frac{n^2 - 1}{2n^2 + 1} \qquad (2)$$

in which $\Delta v = v_{abs} - v_{em}$ stands for the Stokes shift, v_{abs} and v_{em} are the wave numbers of the absorption and the emission, respectively. h is Planck's constant, c is the speed of light in vacuum, a is the Onsager radius. μ_e and μ_g are the permanent dipole moments of the excited state and the ground state, respectively. ε_0 is the permittivity of the vacuum, ε is the static dielectric constant of the solvent, and n is the refractive index, Δf is the orientation polarizability.

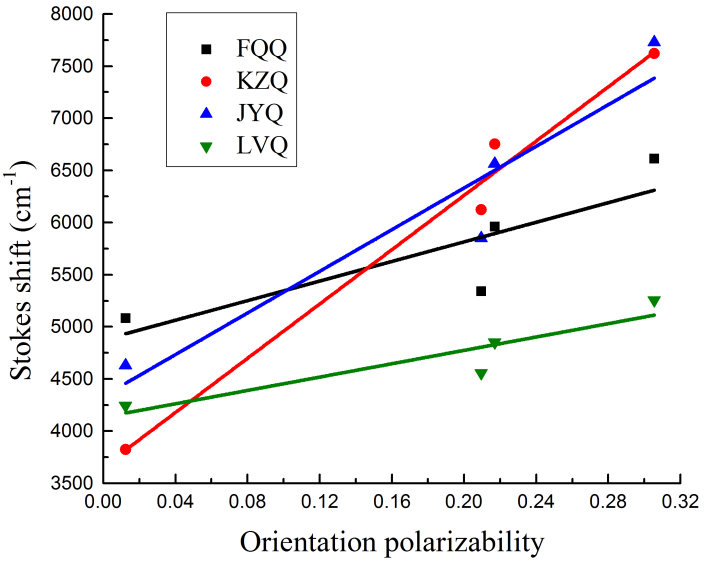

Fig. 4. Lippert-Mataga plots of the target compounds (**KZQ**, **FQQ**, **JYQ**, and **LVQ**).

The plots of Δv as a function of Δf are shown in Fig. 4. According to the Lippert-Mataga equation, the slope of the best-fit line is related to the dipole moment change between the ground state and the excited state ($\mu_e - \mu_g$). The slopes of the four lines are different: 4696, 13012, 9982, and 3201 cm^{-1} for **FQQ**, **KZQ**, **JYQ**, and **LVQ**, respectively. **KZQ** and **JYQ** have much larger slopes than **FQQ** and **LVQ**, which implies larger dipole moment changes for **KZQ** and **JYQ** with

photoexcitation.[28] The large μ_e - μ_g values are beneficial to improving their TPA properties.

2.3. Two-photon properties

The two-photon excited fluorescence (TPEF) spectra of the target compounds in THF and TOL were recorded at different excitation wavelengths (690-950 nm) with a pulse duration of 140 fs at 500 mW. The corresponding two-photon properties are listed in Table 1. The representative TPEF spectra of **KZQ** in THF are shown in Fig. 5 and Fig. 6.

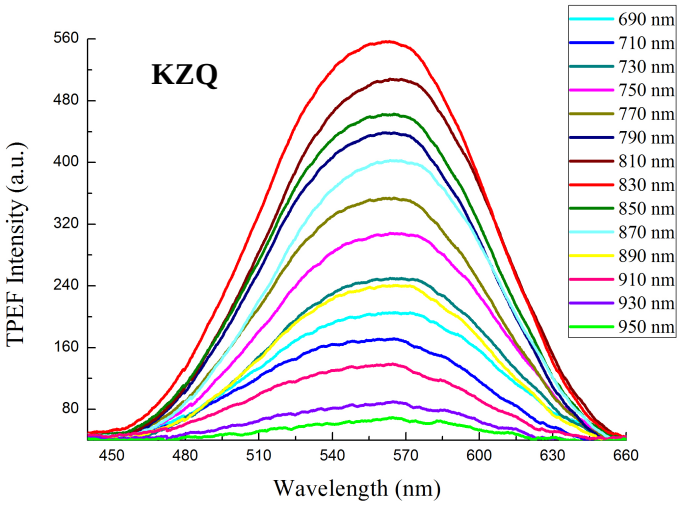

Fig. 5. Two-photon excited fluorescence spectra of **KZQ** in THF ($c = 1\times10^{-3}$ mol L^{-1}) pumped by femtosecond laser pulses at 500 mW under different excitation wavelengths.

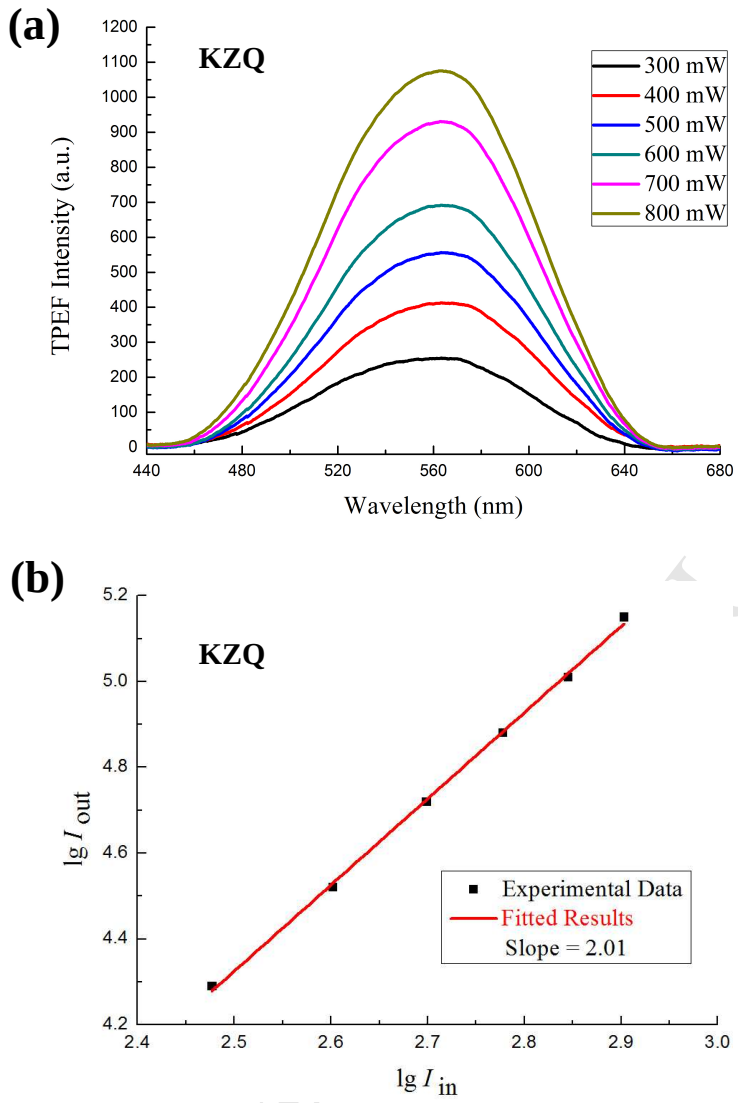

Fig. 6. (a) Two-photon excited fluorescence spectra of **KZQ** in THF (c = 1×10^{-3} mol L^{-1}) at 830 nm under different input powers. (b) Logarithmic plot of the output fluorescence integral (I_{out}) of **KZQ** versus the input laser powers (I_{in}) .

The TPEF spectra of **KZQ** in THF pumped by femtosecond laser pulses at 500 mW under different excitation wavelengths are presented in Fig. 5. One can see that the TPEF intensity is the largest under 830 nm excitation. The optimal excitation wavelengths of the other compounds (**FQQ**, **JYQ**, and **LVQ**) are 830 nm, 790 nm, and 790 nm, respectively. Fig. 6a and Fig. 6b show the fluorescence intensities of **KZQ** under different pump powers and the logarithmic plot of the output

fluorescence integral versus the input powers. As no linear absorption is observed in the range from 500 nm to 1000 nm, the emission excited at 830 nm laser wavelength should be attributed to the TPEF mechanism. The logarithmic plot has a slope of 2.01 as the input laser power is increased, confirming a two-photon excitation mechanism. The other compounds (**FQQ**, **JYQ**, and **LVQ**) are also proved to have the same excitation mechanism.

One can see from Table 1 that the TPEF maximum (λ_{max}^{TPEF}) of **KZQ** in THF is 563 nm, which is evidently red-shifted by 35 nm by comparing with its λ_{max}^{OPEF} (528 nm). The other compounds (**FQQ**, **JYQ**, and **LVQ**) also show 38-51 nm and 35-52 nm red shifts in TOL and THF, respectively. This is attributed to the reabsorption effect[28], which can lead to the energy loss and the red-shift of emission wavelength.

The σ of the target compounds (**FQQ**, **KZQ**, **JYQ**, and **LVQ**) were calculated and presented in Fig. 7 and listed in Table 1. They all have larger σ in THF than in TOL. Obviously, the polarity of solvents has significantly influence on the σ. It is also can be explained by the stronger solute-solvent interaction in THF. The largest σ values in THF (TOL) are 145 GM (118 GM) for **FQQ**, 707 GM (448 GM) for **KZQ**, 286 GM (138 GM) for **JYQ**, and 85 GM (55 GM) for **LVQ**, respectively, which follow the order: **KZQ** > **JYQ** > **FQQ** > **LVQ**. To better understand the relationship between the σ of the target compounds and the distribution of electron densities over the molecules, the density functional theory (DFT) calculations were carried out using the Gaussian 09 program.[30] The nonlocal density function of B3LYP with 6-31G basis sets was used for the calculations. The frontier molecular orbitals of the target compounds were shown in Fig. 8. The HOMO-LUMO energy gaps (ΔE) were calculated and listed in Table 2. Upon excitation, the electron transition from the HOMO to the LUMO is accompanied by the charge transfer from the terminal phenothiazine ring, carbazole ring, and benzene ring to the formyl acceptor. The ΔE of **FQQ**, **KZQ**, **JYQ**, and **LVQ** are 2.65, 2.89, 3.00 and 3.16 eV, respectively. The σ value shows positive correlation with the μ_e - μ_g, but negative correlation with the ΔE. One can see that **LVQ** with A-π-A molecule structure has the smallest μ_e - μ_g (3201

cm^{-1}) and the largest ΔE (3.16 eV). Thus, the charge transfer degree is the weakest, resulting in the smallest σ. Although the ΔE of **FQQ** is 2.65 eV, which is the smallest among the target compounds, the μ_e - μ_g of **FQQ** is much smaller than those of **KZQ** and **JYQ**. Furthermore, **FQQ** has a non-planar molecule structure (Fig. 9), which may weaken the conjugation extension of the whole molecule and reduce the intramolecular charge transfer. Based on the above factors, the σ value of **FQQ** is smaller than those of **KZQ** and **JYQ**. The σ of **KZQ** is nearly 2.5 times as large as that of **JYQ**. This can be explained by the fact that not only the ΔE of **KZQ** is smaller than that of **JYQ**, but the μ_e - μ_g of **KZQ** is larger than that of **JYQ**. The intramolecule charges are almost completely transferred from the carbazole donor to the formyl acceptor. Therefore, **KZQ** shows the largest σ value.

(a)

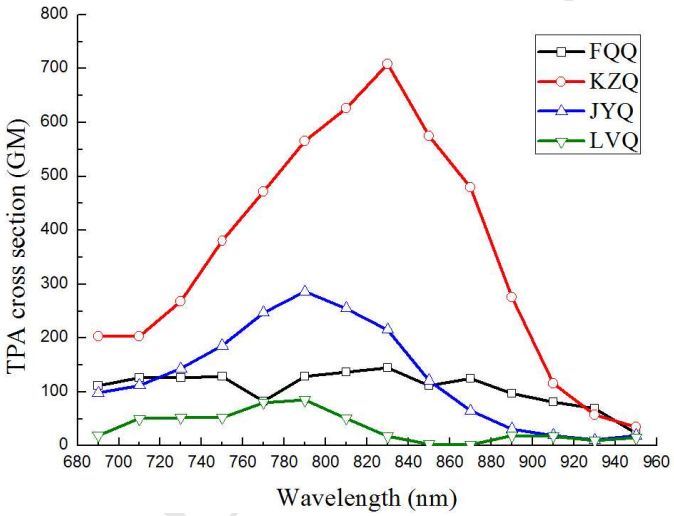

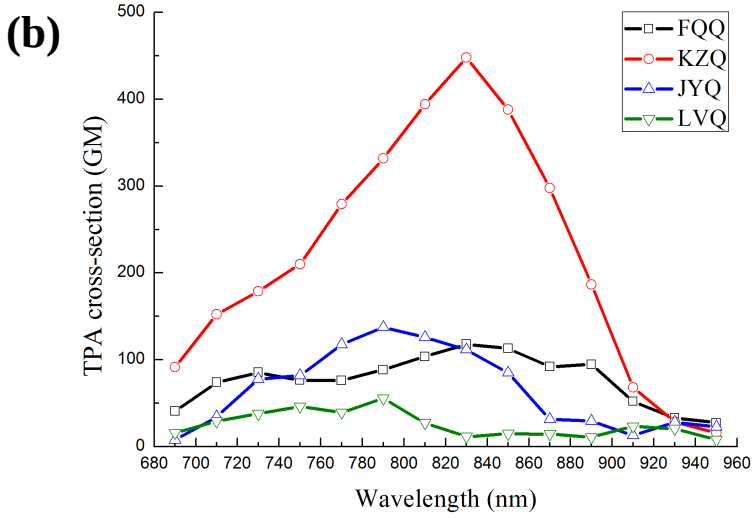

Fig. 7. Two-photon absorption cross-sections of the target compounds (**KZQ**, **FQQ**, **JYQ**, and **LVQ**) in THF (a) and TOL (b) in the 690-950 nm regions.

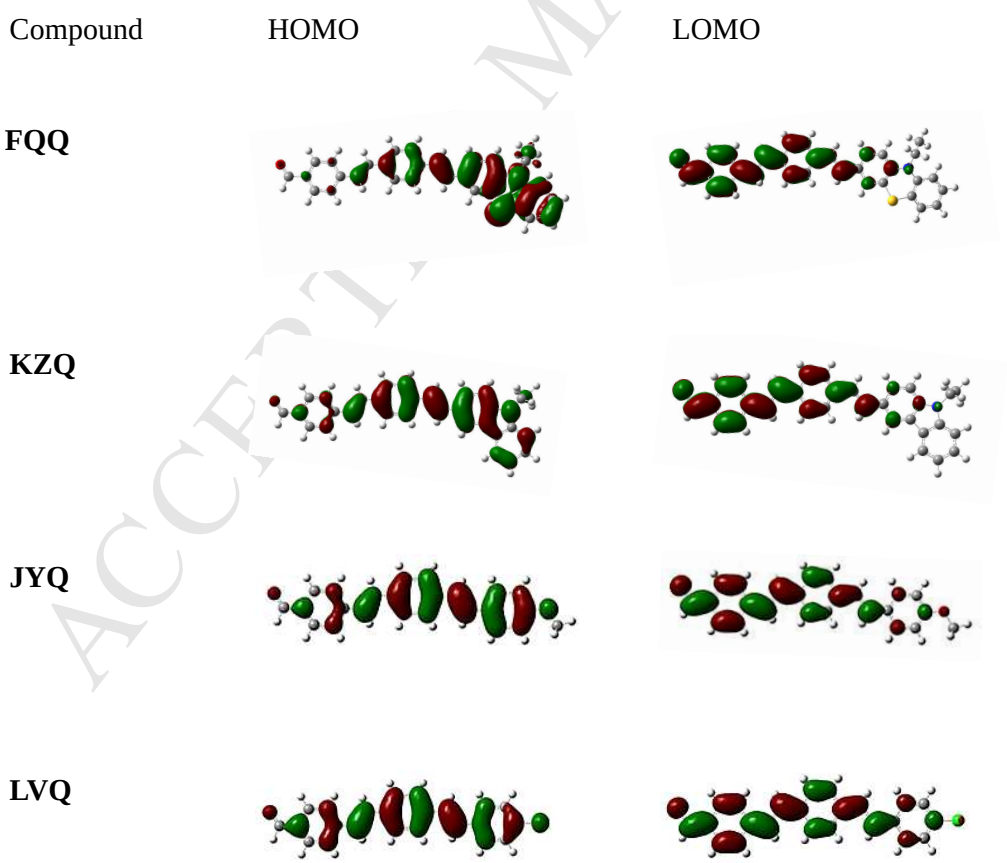

Fig. 8. Frontier molecular orbitals of the target compounds (**FQQ**, **KZQ**, **JYQ**, and **LVQ**).

Table 2. Calculated HOMO, LOMO energy and HOMO-LOMO energy gaps of the target compounds (**FQQ**, **KZQ**, **JYQ**, and **LVQ**).

Compound	HOMO (eV)	LOMO (eV)	HOMO-LOMO energy gaps (eV)
FQQ	-4.86	-2.21	2.65
KZQ	-5.03	-2.14	2.89
JYQ	-5.19	-2.18	3.00
LVQ	-5.52	-2.36	3.16

Compound	Top view	Front view
FQQ	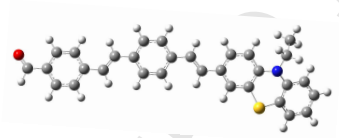	
KZQ	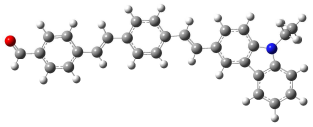	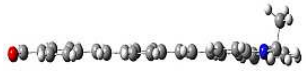
JYQ	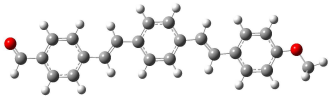	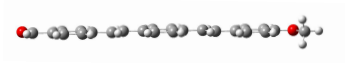
LVQ	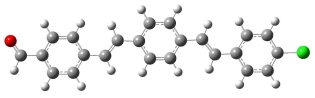	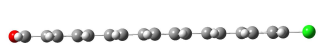

Fig. 9. Optimized geometries of the target compounds (**FQQ**, **KZQ**, **JYQ**, and **LVQ**).

3. Conclusion

In summary, the new donor-π-acceptor / acceptor-π-acceptor compounds (**FQQ**, **KZQ**, **JYQ**, and **LVQ**) were facilely synthesized by Mizoroki-Heck reaction. The important intermediates (**2a**-**2d**) were synthesized by the solvent-free HWE reaction that is simple, safe, and environmentally friendly. Their linear and nonlinear optical properties were systematically investigated in various solvents. The results show that all of the target compounds exhibit obvious solvatochromism and large Stokes shifts. **KZQ** exhibits the excellent optical properties and the σ can be as large as 707 GM in THF, which provide a promising alternative as a polarity-sensitive two-photon fluorescent probe.

4. Experimental section

4.1. General experimental methods

1[22], **1a**[23], **1b**[24], **LSZ**[25] were synthesized according to the literature procedures. DMF and Et_3N were pre-dried over anhydrous magnesium sulfate for 20 h and distilled before use. Other materials were commercially available and were used without further purification. Unless otherwise specified, all the reactions were performed under nitrogen atmosphere using standard Schlenk techniques. ^{1}H NMR spectra were recorded at room temperature on a Bruker AVANCEIII 500 spectrometer in $CDCl_3$ or DMSO-d_6 solvent with tetramethylsilane (TMS) as internal standard. Chemical shifts were reported in δ scale and the standard abbreviations s, d, t, and q refer to singlet, doublet, triplet, and quartet, respectively. Coupling constant (*J*) values are reported in Hertz. FT-IR spectra were measured on KBr pellets with a Thermo Nicolet 6700 spectrometer. Mass spectra were taken on a Therm LCQ TM Deca XP plus ion trap mass spectrometry instrument. Elemental analyses were conducted on a Thermo Finnigan Flash EA 1112 apparatus. Melting points were measured on an X-4 micromelting point apparatus without correction. Column chromatography was

carried out by using silica gel (200-300 mesh) as the stationary phase.

4.2. Optical measurements

The one-photon absorption (OPA) spectra were recorded by a Shimadzu UV-2550 UV-visible spectrometer. The OPEF spectra measurements were performed using a RF-5301PC fluorescence spectrofluorometer with the maximum absorption wavelengths as the excitation wavelengths. The OPA and OPEF spectra of the target compounds (**FQQ**, **KZQ**, **JYQ**, and **LVQ**) were measured in four organic solvents of different polarities. The OPA data were gotten at a concentration of 1×10^{-5} mol L^{-1}, while the OPEF were measured at a concentration of 1×10^{-6} mol L^{-1}. The quartz cuvettes used had a 1 cm path. The Φ was determined by using quinine sulfate (in 0.5 mol L^{-1} H_2SO_4, Φ = 0.546) as the reference according to the literature method.[26] The Φ was corrected as follows:

$$\Phi = \Phi_{ref} \frac{A_{ref}}{A} \frac{n^2}{n_{ref}^2} \frac{F}{F_{ref}} \qquad (3)$$

where the ref subscript stands for the reference molecule, A is the absorbance at λ_{ex}, n is the refractive index of the solution, and F is the integrated area under the corrected emission spectrum.

The σ of the target compounds (**FQQ**, **KZQ**, **JYQ**, and **LVQ**) were obtained by the TPEF method with a femtosecond laser pulse and a Ti : sapphire system (680-1080 nm, 80 MHz, 140 fs) as the light source. The samples were dissolved in THF and TOL at a concentration of 1×10^{-3} mol L^{-1}. The intensities of the TPEF spectra of the reference and the samples were determined at their excitation wavelengths. Thus, the σ of the samples were determined by the following equation:

$$\sigma = \sigma_{ref} \frac{\Phi_{ref}}{\Phi} \frac{n_{ref}}{n} \frac{c_{ref}}{c} \frac{F}{F_{ref}} \qquad (4)$$

where the ref subscript stands for the reference molecule, σ is the TPA cross-section (here fluorescein in 0.1 mol L^{-1} sodium hydroxide solution at a concentration of 1×10^{-3} mol L^{-1} is used as reference, σ = 36 GM)[31]. n is the refractive index of the

solution, *c* is the concentration of the solution, *F* is the integrated area under the corrected emission spectrum, and *Φ* is the fluorescence quantum yield.

4.3. General procedure for the preparation of 2a-2d

*4.3.1 3-[(1E)-2-(4-ethenylphenyl)ethenyl]-10-ethyl-10H-phenothiazine (**2a**).* **LSZ** (2.54 g, 10 mmol), t-BuOK (2.24 g, 20 mmol) and **1a** (3.83 g, 15 mmol) were placed in a grinding jar and mixed. Then the grinding jar was placed in a planetary ball-mill and stirred with a 7 mm stainless steel balls at 550 runs per minute during 2 h at room temperature. Then 60 mL CH_2Cl_2 was added in the jar and the mixture was first washed twice with 200 mL water, then saturated brine and dried over anhydrous magnesium sulfate. The solvent was removed under reduced pressure and the residue was purified by silica-gel column chromatography (V_{PE} : V_{EA} = 10 : 1) to afford **2a** as bright yellow needle crystals. Yield: 71.2% (2.52 g). m.p. 134-135℃; ^{1}H NMR (DMSO-d_6, 500 MHZ) *δ*: 7.55 (d, *J* = 8.3 Hz, 2H), 7.47 (d, *J* = 8.3 Hz, 2H), 7.41 (dd, J_1 = 7.8 Hz, J_2 = 1.9 Hz, 1H), 7.40 (s, 1H), 7.21 (t, *J* = 7.8 Hz, 1H), 7.17 (d, *J* = 16.5 Hz, 1H), 7.15 (dd, J_1 = 7.6 Hz, J_2 = 1.4 Hz, 1H), 7.13 (d, *J* = 16.5 Hz, 1H), 7.03 (d, *J* = 7.8 Hz, 1H), 7.01 (d, *J* = 7.8 Hz, 1H), 6.95 (t, *J* = 7.5 Hz, 1H), 6.73 (dd, J_1 = 17.6 Hz, J_2 = 11.0 Hz, 1H), 5.85 (d, *J* = 17.7 Hz, 1H), 5.26 (d, *J* = 11.1 Hz, 1H), 3.93 (q, 2H), 1.31 (t, *J* = 6.8 Hz, 3H); FT-IR (KBr) *v*: 3048, 2964, 2854, 1598, 1571, 1463, 1324, 1237, 1134, 964, 828, 745 cm^{-1}; ESI-MS *m/z*: 356.1 $[M+H]^+$; Anal. calcd for $C_{24}H_{21}NS$: C 81.09, H 5.95, N 3.94; found C 81.36, H 6.08, N 4.13.

*4.3.2 3-[(1E)-2-(4-ethenylphenyl)ethenyl]-9-ethyl-9H-carbazole (**2b**).* The synthesis of this compound was similar to **2a**. Off-white crystalline powder. Yield: 74.4% (2.40 g). m.p. 140-141 ℃; ^{1}H NMR (DMSO-d_6，500MHz) *δ*: 8.41 (s, 1H), 8.19 (d, *J* = 7.7 Hz, 1H), 7.76 (d, *J* = 8.5 Hz, 1H), 7.62 (d, *J* = 8.2 Hz, 2H), 7.61 (d, *J* = 8.5 Hz, 2H), 7.50 (d, *J* = 8.2 Hz, 2H), 7.48 (t, *J* = 7.5 Hz, 1H), 7.45 (d, *J* = 16.4 Hz, 1H), 7.28 (d, *J* = 16.4 Hz, 1H), 7.23 (t, *J* = 7.4 Hz, 1H), 6.75 (dd, J_1 = 17.6 Hz, J_2 = 10.9 Hz, 1H), 5.86 (d, *J* = 17.7 Hz, 1H), 5.26 (d, *J* = 11.0 Hz, 1H), 4.46 (q, 2H), 1.33 (t, *J* = 7.1 Hz, 3H); FT-IR (KBr) *v*: 3019, 2931, 2886, 1624, 1594, 1475, 1336, 1234, 1155,

968, 826, 748, 608 cm^{-1}; ESI-MS *m/z*: 324.3 $[M+H]^+$; Anal. calcd for $C_{24}H_{21}N$: C 89.12, H 6.54, N 4.33; found C 89.25, H 6.58, N 4.42.

*4.3.3 1-ethenyl-4-[(1E)-2-(4-methoxyphenyl)ethenyl]benzene (**2c**).* The synthesis of this compound was similar to **2a**. Light yellow flaky crystal. Yield: 80.6% (1.91 g). m.p. 149-151 ℃; ^1H NMR (DMSO-d_6, 500MHz) δ: 7.54 (d, J = 8.7 Hz, 4H), 7.46 (d, J = 8.3 Hz, 2H), 7.21 (d, J = 16.5 Hz, 1H), 7.09 (d, J = 16.5 Hz, 1H), 6.95 (d, J = 8.7 Hz, 2H), 6.73 (dd, J_1 = 17.7 Hz, J_2 = 11.0 Hz, 1H), 5.84 (dd, J_1 = 17.7 Hz, J_2 = 0.6 Hz, 1H), 5.26 (dd, J_1 = 11.0 Hz, J_2 = 0.6 Hz, 1H), 3.78 (s, 3H); FT-IR (KBr) v: 3000, 2954, 2835, 1601, 1512, 1249, 1176, 1034, 968, 837, 535 cm^{-1}; ESI-MS *m/z*: 237.3 $[M+H]^+$; Anal. calcd for $C_{17}H_{16}O$: C 86.40, H 6.82; found C 86.69, H 6.97.

*4.3.4 1-chloro-4-[(1E)-2-(4-ethenylphenyl)ethenyl]benzene (**2d**).* The synthesis of this compound was similar to **2a**. Light yellow flaky crystal. Yield: 74.8% (1.11 g). m.p. 164-165 ℃; ^1H NMR (DMSO-d_6, 500MHz) δ: 7.64 (d, J = 8.5 Hz, 2H), 7.60 (d, J = 8.3 Hz, 2H), 7.50 (d, J = 8.3 Hz, 2H), 7.44 (d, J = 8.5 Hz, 2H), 7.29 (s, 2H), 6.75 (dd, J_1 = 17.6 Hz, J_2 = 11.0 Hz, 1H), 5.87 (dd, J_1 = 17.6 Hz, J_2 = 0.7 Hz, 1H), 5.28 (dd, J_1 = 11.0 Hz, J_2 = 0.7 Hz, 1H); FT-IR (KBr) v: 3017, 1626, 1509, 1488, 1408, 1094, 971, 839, 523 cm^{-1}; ESI-MS *m/z*: 241.2 $[M+H]^+$; Anal. calcd for $C_{16}H_{13}Cl$: C 79.83, H 5.44; found C 80.06, H 5.62.

4.4. General procedure for the preparation of the target compounds (**FQQ**, **KZQ**, **JYQ**, **and LVQ**)

*4.4.1 3-[(1E)-2-[4-[(1E)-2-(4-formylphenyl)ethenyl]phenyl]ethenyl]-10-ethyl-10H-phenothiazine (**FQQ**).* A mixture of **2a** (0.36 g, 1 mmol), 4-bromobenzaldehyde (0.18 g, 1 mmol), $Pd(OAc)_2$ (0.007 g, 0.03 mmol), and tri-*o*-tolylphosphine (0.04 g, 0.13 mmol) in DMF / Et_3N was stirred under N_2 at 120 ℃ for 20 h. After cooling, the mixture was poured into the ice water and filtered. The residue was purified by silica-gel column chromatography (V_{PE} : V_{EA} = 15 : 1) to afford **FQQ** as orange-red crystalline powder. Yield: 60.5% (0.28 g). m.p. 204-206 ℃; ^1H NMR (DMSO-d_6, 500MHz) δ: 9.99 (s, 1H), 7.92 (d, J = 8.3 Hz, 2H), 7.84 (d, J = 8.3 Hz, 2H), 7.67 (d, J = 8.3 Hz,

2H), 7.61 (d, J = 8.3 Hz, 2H), 7.50 (d, J = 16.5 Hz, 1H), 7.43 (dd, J_1 = 7.8 Hz, J_2 = 2.0 Hz, 1H), 7.42 (s, 1H), 7.40 (d, J = 16.5 Hz, 1H), 7.23 (d, J = 16.4 Hz, 1H), 7.21 (t, J = 7.8 Hz, 1H), 7.17 (d, J = 16.4 Hz, 1H), 7.15 (dd, J_1 = 7.6 Hz, J_2 = 1.4 Hz, 1H), 7.03 (d, J = 7.8 Hz, 1H), 7.02 (d, J = 7.8 Hz, 1H), 6.95 (t, J = 7.4 Hz, 1H), 3.94 (q, 2H), 1.32 (t, J = 6.9 Hz, 3H); FT-IR (KBr) v: 3022, 2924, 2853, 1693, 1594, 1570, 1466, 1331, 1248, 1165, 964, 827, 751 cm^{-1}; ESI-MS m/z: 460.4 $[M+H]^+$; Anal. calcd for $C_{31}H_{25}NOS$: C 81.01, H 5.48, N 3.05; found C 81.19, H 5.53, N 3.32.

*4.4.2 3-[(1E)-2-[4-[(1E)-2-(4-formylphenyl)ethenyl]phenyl]ethenyl]-9-ethyl-9H-carbazole (**KZQ**).* The synthesis of this compound was similar to **FQQ**. Yellow crystalline powder. Yield : 67.2% (0.29 g). m.p. 222-224 ℃; ^{1}H NMR (DMSO-d_6, 500MHz) δ: 10.00 (s, 1H), 8.43 (s, 1H), 8.20 (d, J = 7.7 Hz, 1H), 7.93 (d, J = 8.3 Hz, 2H), 7.85 (d, J = 8.3 Hz, 2H), 7.78 (d, J = 8.6 Hz, 1H), 7.70 (d, J = 8.5 Hz, 2H), 7.67 (d, J = 8.5 Hz, 2H), 7.64 (d, J = 8.5 Hz, 1H), 7.63 (d, J = 8.2 Hz, 1H), 7.52 (d, J = 16.4 Hz, 1H), 7.51 (d, J = 16.3 Hz, 1H), 7.48 (t, J = 7.5 Hz, 1H), 7.41 (d, J = 16.4 Hz, 1H), 7.31 (d, J = 16.3 Hz, 1H), 7.24 (t, J = 7.4 Hz, 1H), 4.47 (q, 2H), 1.34 (t, J = 7.1 Hz, 3H); FT-IR (KBr) v: 3023, 2930, 2889, 1696, 1623, 1588, 1473, 1335, 1234, 1166, 966, 824, 748, 611 cm^{-1}; ESI-MS m/z: 428.3 $[M+H]^+$; Anal. calcd for $C_{31}H_{25}NO$: C 87.09, H 5.89, N 3.28; found C 87.24, H 5.92, N 3.47.

*4.4.3 4-[(1E)-2-[4-[(1E)-2-(4-methoxyphenyl)ethenyl]phenyl]ethenyl]benzaldehyde (**JYQ**).* The synthesis of this compound was similar to **FQQ**. Yellow crystalline powder. Yield: 72.8% (0.25 g). m.p. 254-256 ℃; ^{1}H NMR (DMSO-d_6, 500MHz) δ: 9.99 (s, 1H), 7.92 (d, J = 8.2 Hz, 2H), 7.84 (d, J = 8.2 Hz, 2H), 7.67 (d, J = 8.4 Hz, 2H), 7.62 (d, J = 8.4 Hz, 2H), 7.57 (d, J = 8.7 Hz, 2H), 7.50 (d, J = 16.5 Hz, 1H), 7.40 (d, J = 16.5 Hz, 1H), 7.28 (d, J = 16.4 Hz, 1H), 7.13 (d, J = 16.4 Hz, 1H), 6.97 (d, J = 8.7 Hz, 2H), 3.79 (s, 3H); FT-IR (KBr) v: 3021, 2919, 2848, 1698, 1589, 1512, 1254, 1171, 1030, 967, 834, 548 cm^{-1}; ESI-MS m/z: 341.2 $[M+H]^+$; Anal. calcd for $C_{24}H_{20}O_2$: C 84.68, H 5.92; found C 84.75, H 6.02.

*4.4.4 4-[(1E)-2-[4-[(1E)-2-(4-chlorophenyl)ethenyl]phenyl]ethenyl]benzaldehyde (**LVQ**).* The synthesis of this compound was similar to **FQQ**. Yellow crystalline

powder. Yield: 70.6% (0.24 g). m.p. 248-250 ℃; ^{1}H NMR (DMSO-d_6，500MHz) δ: 10.00 (s, 1H), 7.93 (d, J = 8.3 Hz, 2H), 7.85 (d, J = 8.3 Hz, 2H), 7.70 (d, J = 8.4 Hz, 2H), 7.66 (d, J = 8.4 Hz, 2H), 7.65 (d, J = 8.5 Hz, 2H), 7.51 (d, J = 16.5 Hz, 1H), 7.46 (d, J = 8.5 Hz, 2H), 7.42 (d, J = 16.5 Hz, 1H), 7.33 (s, 2H); FT-IR (KBr) v: 3021, 1700, 1597, 1488, 1419, 1166, 1091, 968, 832, 545 cm^{-1}; ESI-MS m/z: 345.3 $[M+H]^+$; Anal. calcd for $C_{23}H_{17}ClO$: C 80.11, H 4.97; found C 80.36, H 5.08.

Acknowledge

We are grateful to the Natural Science Foundation of Zhejiang province, China (Grant No. LY15B030006) and the National Natural Science Foundation of China (Grant No. 21103151) for financial support.

References and notes

1. (a) Ai, J.; Li, J.; Lu, G.; Yun, G. H.; Xu, L.; Wang, E. K. *Sens. Actuators, B* **2016**, *222*, 918-922. (b) Qing, S. M.; (b) Mei, Q. S.; Jing, H. R.; Li, Y.; Yisibashaer, W.; Chen, J.; Li, B. N.; Zhang, Y. *Biosens. Bioelectron.* **2016**, *75*, 427-432.
2. Dey, R. Y.; Rai, V. K. *Spectrochim. Acta, Part A* **2015**, *151*, 213-217.
3. (a) Li, L.; Wang, P.; Hu, Y. L.; Lin, G.; Wu, Y. Q.; Huang, W. H.; Zhao, Q. Z. *Spectrochim. Acta, Part A* **2015**, *139*, 243-252. (b) Yang, Y.; Tian, H. P.; Yang, D. Q.; Wu, N. N.; Zhou, J.; Liu, Q.; Ji, Y. F. *Sens. Actuators, A* **2014**, *209*, 33-40.
4. (a) Dong, Y.; Wang, G. L.; Ni, H. Q.; Chen, J. H.; Gao, F. Q.; Li, B. C.; Pei, K. M.; Niu, Z. C. *Opt. Commun.* **2015**, *355*, 274-278. (b) Ca, N. X.; Lien, V. K.; Nghia, N. X.; Chi, T. K.; Phan, T. L. *Nanotechnology* **2015**, *26*, 445701.
5. (a) Velusamy, M.; Shem, J. Y.; Lin, J. T.; Lin, Y. C.; Hsiech, C. C.; Lai, C. H.; Lai, Y. C.; Hu, M. L.; Chen, Y. C.; Chou, P. T.; Hsiao, J. K. *Adv. Funct. Mater*. **2009**, *19*, 2388. (b) Guo, Y. Y.; Seki, K.; Miyamoto, K. I.; Wagner, T.; Michael, J. S.; Yoshinobu, T. *Procedia Engineering* **2014**, *87*, 456-459.
6. (a) Du, Y. B.; Lin, X. D.; Jia, T. J.; Dong, J. *Opt. Commun.* **2015**, *338*, 257-260. (b)

Varun, K.; Protasis, P.; Thank, C *Phys. Chem. Chem. Phys.* **2015**, *17*, 12299.

7. Druzhinin, S. K.; Galievsky, V. A.; Demeter, A.; Kovalenko, S. A.; Senyushkina, T.; Dubbaka, S. R.; Knoche, P.; Mayer, P.; Grosse, C.; Stalke, D. *J. Phys. Chem. A* **2015**, *119*, 11820-11836.
8. Priya, J.; Samarendra, P. S. *J. Phys. Chem. C* **2015**, *119*, 14890-14899.
9. Achelle, S.; Ple, N.; Turck, A. *Res. Advances* **2011**, *1*, 364-388.
10. (a) Lan, S. C.; Raghunath, P.; Lu, Y. H.; Wang, Y. C.; Lin, S. W.; Liu, C. M.; Jiang, J. M.; Lin, M. C.; Wei, K. H. *ACS Appl. Mater. Interfaces* **2014**, *6*, 9298-9306.
11. (a) Okino, S.; Takaya, T.; Iwata, K. *Chem. Lett.* **2015**, *44*, 1059-1061. (b) Do, K.; Cho, N.; Siddiqui, S. A.; Singh, S. P.; Sharma, G. D.; Ko, J. *Dyes Pigm.* **2015**, *120*, 126-135.
12. (a) Stephane, A. B.; Cecile, M.; Karine, H.; Marc, F; Patrick, B.; Philippe, M.; Pascale, A. -S. *J. Solid State Chem.* **2002**, *168*, 668-674. (b) Sudipta, D.; Durga, S. C.; Madhusudan, B.; Abhinandan, R.; Nicol, G.; Ennio, Z. *Inorg. Chim. Acta* **2010**, *363*, 3700-3705.
13. Andreas, L.; Li, Z. H.; Alhama, A. -E.; Ai, F. L.; Marcel, G.; Vladimir, S.; Matthias, S.; Frank, W. *Adv. Funct. Mater*. **2015**, *25*, 44-57.
14. Kimihiro, S.; Jonathan, A. N.; Jie, R. Z.; David, N. B.; Arjun, G. Y.; Michael, J. T. *J. Phys. Chem. A* **2011**, *115*, 5525-5539.
15. Oliva, M. M.; Juárez, R.; Ramos, M.; Segura, J. L.; Cleuvenbergen, S. V.; Clays, K. *J. Phys. Chem. C* **2013**, *117*, 626.
16. Harry, M. W.; Bhaskar, A.; Ramakrishna, G.; GoodsonIII, T. ; Imamura, M.; Mawatari, M. *J. Am. Chem. Soc.* **2008**, *130*, 3252.
17. Dumrath, C.; Dumrath, A.; Neumann, H.; Beller, M.; Kedyrov, R. *ChemCatChem.* **2014**, *6*, 3101-3104.
18. Wan, Z. Q.; Jia, C. Y.; Duan, Y. D.; Zhou, L. L.; Lin, Y.; Shi, Y. *J. Mater. Chem.* **2012**, *42*, 25140-25147.
19. (a) Jin, F.; Cai, Z. B.; Huang, J. Q.; Sheng, L. L.; Tian, Y. P. *J. Mol. Struct.* **2015**, *1093*, 33-38. (b) Cai, Z. B.; Liu, L. F.; Kong, C.; Zhu, Y. X. *Acta Phys. -Chim. Sin.* **2014**, *30*, 164-170.

20. (a) Polander, L. E.; Pandey, L.; Barlow, S.; Tiwari, S. P.; Risko, C. B.; Kippelen, C. *J. Phys. Chem. C* **2011**, *115*, 23149. (b) Beverina, L.; Fu, J.; Leclercq, A.; Zojer, E.; Pacher, P.; Barlow, S. *J. Am. Chem. Soc.* **2005**, *12*, 7282.
21. (a) Andrzej, E.; Piotr, K. J. *Phys. Chem. B* **2015**, 119, 13185-13197. (b) Mihir, G.; Subrata, S. *Spectrochim. Acta, Part A* **2015**, *150*, 959-965.
22. Zhao, S. H.; Kang, J.; Swapan, C.; Du, Y. T.; Kang, J. Y.; Zhao, X, N.; Xu, Y. F.; Chen, R. X.; Wang, Q. Q.; Shi, X. T. *J. Heterocyclic Chem.* **2014**, *51*, 683.
23. (a) Venkatesan, K.; Satyanarayana, V. V.; Mohanapriya, K.; Khora, S. S.; Sivakumar, A. *Res. Chem. Intermed.* **2015**, *41*, 595-607. (b) Dumitrascu, A.; Howell, B. A. *Polym. Degrad. Stab.* **2011**, *96*, 342-349.
24. Hu, R. T.; Lv, L. F.; Ruan, B. F.; Wang, P.; Zhang, M. L.; Zhou, H. P.; Li, S. L.; Wu, J. Y.; Tian, Y. P. *Sci. China, Ser. B* **2009**, *52*, 1210-1215.
25. (a) Boutevin, B.; Hamoui, B.; Parisi, J. -P.; Ame´duri, B. *Eur. Polym. J.* **1996**, *32*, 159-163. (b) Carbonneau, C.; Frantz, R.; Durand, J. -O.; Lanneau, G. F.; Corriu, R. J. P. *Tetrahedron Lett.* **1999**, *40*, 5855-5858.
26. Demas , J. N.; Crosby, G. A. *J. Phys. Chem.* **1971**, *75*, 991-1024.
27. Patel, S. A.; Cozzuol, M.; Hales, J. M.; Richards, C. I.; Sartin, M.; Hsiang, J. C.; Vosch, T.; Perry , J. W.; Dickson, R. M. *J. Phys. Chem. C* **2009**, *113*, 20264.
28. Ji, S. M.; Yang, J.; Yang, Q.; Liu, S. S.; Chen, M. D.; Zhao, J. Z. *J. Org. Chem.* **2009**, *74*, 4855.
29. Ren, Y.; Fang, Q.; Yu, W. T.; Lei, H.; Tian, Y. P.; Jiang, M. H. *J. Mater. Chem.* **2000**, *10*, 2025.
30. Sylwia, O. -J.; Katarzyna, S.; Malgorzata, K.; Jozef, L. *J. Mol. Struc-theochem*. **2009**, *911*, 1-7.
31. Albota, M. A.; Xu, C.; Webb, W. W. *Appl. Opt*. **1998**, *37*, 7352.